Soft Matter

Accepted Manuscript

ROYAL SOCIETY OF CHEMISTRY

www.rsc.org/softmatter

Soft Matter

RSCPublishing

ARTICLE

Oscillations in modulus in solutions of graphene oxide and reduced graphene oxide with grafted poly-N-isopropylamide

Cite this: DOI: 10.1039/x0xx00000x

Received 00th January 2012,
Accepted 00th January 2012

DOI: 10.1039/x0xx00000x

www.rsc.org/

Saud Hashmi[a,d,e,#], Amin GhavamiNejad [d,f#], Florian J. Stadler[a,b,c,d,g*], Dongmei Wu[h,*]

In a material consisting of graphene oxide or reduced graphene oxide and poly-N-isopropylamide (PNIPAM) in aqueous solution, a new type of rheological behaviour is found. When subjecting the material to a short and relatively small deformation pulse, the modulus, observed by small deformations in the linear-viscoelastic or very slightly nonlinear range, oscillates with periodicities between 100 and several 1000 seconds, while in many cases also increasing systematically. The periodicity depends on filler-content and on sample preparation method (in-situ polymerisation vs. blending). When subjecting the material to strongly nonlinear deformations (γ_0=100-300%), the resulting linear viscoelastic behaviour changes from a periodic oscillation to a quick recovery of the original data, followed by a decrease and a subsequent increase beyond the value of the modulus of the material prior to the deformation pulse.

Introduction

Recently graphene and graphene oxide have gained great scientific attention due to their attractive electronic, catalytic, mechanical, optical, and magnetic properties, which have great potential in various applications ranging from energy storage to biomedical materials.[1-3] Graphene oxide (GO) is often used as an intermediate of graphene production and contains various oxygen containing groups (primarily hydroxyl and epoxy groups),[1, 2] which make GO hydrophilic and, therefore, useful for applications in polar matrices and solvents such as water.[3] As the oxygen concentration is highest at the edges of the GO-sheets and lowest in the centre, GO behaves like an amphiphile.[4-7] Furthermore, the oxygen-containing groups also facilitate grafting, which is potentially useful in colloids, liquid crystals, gels, amphiphiles, membranes, foams, and polymeric materials; interest in these areas is primarily driven by the fact that graphene and GO have the purest 2D-structure available.[1, 8-14] As GO is not electrically conductive and, furthermore, for some applications has too many oxygen groups on the surface, GO is reduced, yielding RGO.

Recently, composites of stimuli responsive polymers and GO have produced multi responsive, cost effective, and structurally defined soft materials with improved physical properties.[8, 15] Different routes to grafting poly-N-isopropylamide (PNIPAM) onto GO were explored including free radical polymerisation.[16-19] While some practical applications have been developed already, an understanding of the dynamics, behaviour, and structure of these materials is still incomplete.

The rheological behaviour of composite polymer melts and solutions has been studied for a long time due to their importance in practice.[20-23] The properties of nanocomposites in comparison to classical microcomposites are of great interest, as the former have a considerably larger surface area due to their nano-size, making surface interactions a significantly more important factor. While nanofillers are generally more effective than microfillers in terms of e.g. modifying rheological properties (e.g., decreasing the nonlinearity limit,[20, 24-26]) the use of sheet-like nanofillers, such as nanoclays and graphene or GO has the additional consequence of confining neighbouring polymer chains,[24, 27, 28] which changes the chain dynamics by forcing them in one- or two-dimensional channels. PNIPAM itself has been the subject of intensive investigations due to its thermosensitivity,[29, 30] which can be tuned by copolymerisation with more or less hydrophobic copolymers and the addition of salt.[31-34] PNIPAM and its copolymers have also been investigated for its application in hydrogels, where a special focus was put on improving the mechanical strength.[35-39]

The term *rheochaos* has been used quite *chaotically* in literature. While the literature agrees on using the term for oscillations in rheological properties (usually viscosity) as a function of time, there is disagreement on what is considered to be chaotic and what is not. For instance, some researchers[40, 41]

use the term for fluctuations in viscosity with a certain periodicity – the oscillations observed are not pure sinusoidal oscillations, but the viscosity fluctuates with a period fixed the sample and the experimental setup, typically in the order of seconds to minutes. However, some scientists[42] only use the term for statistical oscillations without a recognizable periodicity.

Reports on rheochaos so far, using the broader definition, have described complex fluids like wormlike micellar solutions[40, 42, 43] and cylinder-, onion- or spherical- aggregates.[41, 44, 45] Rheochaos was only reported to occur under continuous shear conditions at intermediate shear rates, $\dot{\gamma}$, typically in the range of 10-100 rad/s. Explanations for rheochaos were proposed to be cascades of slip movements.[46] Concentrated polymer solutions and other related complex fluids can usually be rheologically characterized conveniently in this range, but it does not mean that this shear rate range is actually representative.

Considering the significant amounts of partially contradictory literature on the topic of rheochaos, it is intended to check how complex composite materials based on PNIPAM grafted on GO and RGO behave under mildly nonlinear deformation, which have not been investigated previously by such rheological experiments. Unusual oscillations in rheological behaviour are tested for periodicity and how they relate to applied rheological conditions and material composition. The ultimate aim is to test for conditions, under which an anomalous rheological behaviour is observed, which could help shedding light on the structure of these composites as well as on the topic of rheochaos in general.

Experimental

Synthesis

The synthesis of the samples has been published by Ghavaminejad et al..[26] In brief, GO was synthesized according to a modified Hummer's method[50] and reduced to RGO by hydrazine hydrate as described by Ghavaminejad et al.[26] The resulting GO- and RGO-sheets had predominantly a thickness of a single graphene layer with some wrinkles typical for RGO. The size of the sheets is typically in the range of several μm in various odd shapes.

The polymer concentration was set to be 6.25 w/v% for all samples, which corresponds to 5.88 wt.% PNIPAM-content for a sample without filler and 5.87 wt.% for 3 wt.% filler. The sample designation, e.g. PNI-GO3, means that 3 w/w% (with respect to the PNIPAM concentration) was added, which corresponds to a GO concentration of 0.176 wt.% with respect to the whole sample.

To synthesize the PNIPAM, N,N,N',N'-tetramethylethylenediamine (TMEDA, Fluka,>99%, 1 mmol/mL) and ammonium peroxodisulfate (APS, Aldrich, >98%, 10 mmol/mL)) were mixed with purified NIPAM[26] and the fillers (GO or RGO) in ultrapure H_2O at 10°C and *in situ* polymerised radically for 24h. PNI+GO3blend sample was produced by mixing 500 mg PNIPAM made with the abovementioned method with 15 mg of GO. Hence, two different types of composite samples were produced – *in-situ* synthesized composites (PNI-GO2, PNI-GO3, PNI-RGO3) and a physical blend (PNI+GO3blend).

Because of the fillers, it is not possible to determine the molar mass distribution by chromatographic means, however, measurements of pure PNIPAM (PNI) made with the same method lead to a molar mass M_w=3 200 kg/mol and M_w/M_n=5.3 using a GPC (Agilent 1200 with PL gel 10mm guard column and two PL gel Mixed-B 10 mm columns with dimethylformamide as solvent).[51] This PNIPAM was also used for the PNI+GO3blend. It is, therefore, safe to assume that the *in-situ* polymerised composites also have a very high molar mass, which means that the PNIPAM is entangled despite the low concentration.

Table 1: Composition of the PNIPAM-composites

Sample	Graphene Oxide [wt.%]a	Graphene Oxide [mg]	Filler concentration [wt.% of total sample]
PNI-GO2	2	10	0.118
PNI-GO3	3	15	0.176
PNI-RGO3 [b]	3	15	0.176
PNI+GO3blend	3	15	0.176
PNI	0	0	0

[a] with respect to PNIPAM.

[b] In this sample RGO was used as filler.

Ghavaminejad et al.[26] proved the grafting of PNIPAM on the GO-sheets by transmission electron microscopy (TEM), X-ray diffraction (XRD), thermogravimetry (TGA), and RAMAN-spectroscopy. However, while it is clear from abovementioned data that the degree of grafting is significant but not quantifiable. Rheological data[26] suggest that the sample PNI-GO3 has solid-like characteristics, while the other samples show some solid-like characteristics, but mostly viscoelastic-like behaviour.

Because the samples are suspensions, it is important to check whether they are stable. Figure 1 shows a photograph of one of the samples after 17 months, among which the sample was kept standing in a corner in the lab and not touched for the last 12 months. It is obvious that even after such a long time, it is not possible to see signs of settling of the GO, proving the stability of the suspensions. Obviously, the higher the GO-content, the higher the viscosity (up to $\eta_0 \rightarrow \infty$ for the gel-like samples) and, thus, the lower the tendency to settle.

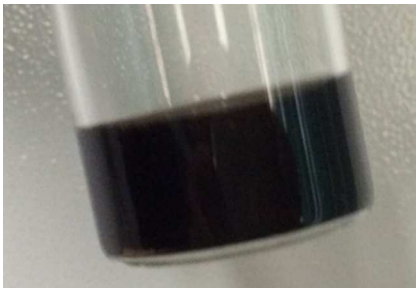

Figure 1: photograph of sample PNI-GO0.25 after 17 months.

Results

Rheology

Two rheometers were used for the rheological characterization of the samples. All experiments shown in the article were carried out on a Malvern Kinexus Pro using a Peltier heated chamber with a 20 or 50mm/1° cone and plate setup. For all measurements a test temperature of 25°C was used and the sample chamber's atmosphere was saturated with H_2O-vapor

and contained by liquid seals. For definitely excluding a strange rheometer artefact, some tests were run on a Paar Physica MCR 301 using a 25 mm parallel plate setup, however, without proper solvent control. The results were found to qualitatively agree to the ones obtained by Malvern Kinexus Pro discussed in this article, but because of the insufficient solvent control, it is not possible to make a quantitative comparison. Ghavaminejad et al.[26] previously proved that 25°C is sufficiently below the lower critical solution temperature (LCST) of the composites to avoid any influence of this transition, which occurs around 33°C.[31, 52-54]

The samples were subjected to first a strain sweep, a test at a constant frequency ω of 10 rad/s, where the deformation amplitude was increased from γ_0=0.1% to a deformation γ_0^{max}, which was varied from 3% to 100%. For each sample, several different maximum deformations γ_0^{max} were applied. This test was immediately followed by a time sweep, a test at constant frequency ω of 10 rad/s and shear stress τ of 2 Pa (lower shear stresses would not allow for a reliable measurement of phase angle δ) lasting 10000 s or longer. The data was collected every 1 s. The resulting deformation γ_0 is close to the border of the lve to nonlinear regime, but it is still linear. Due to the low stiffness of the samples, using lower strains would lead to significantly worse signals. While it would be interesting to have a close look at the raw data and to analyse them, the setup used unfortunately does not allow for this. While PNIPAM is often used as a thermosensitive material, we will not investigate this property in this article.

The oscillations in the data were analysed two different ways. Firstly, the data was analysed by FFT with polynomials of degree 3-10 subtracted and normalized by the average value of the whole dataset.

$$G_{norm}(t) = \sum_{i=3}^{10} \frac{|G^*|(t) - P_i}{mean(|G^*|(t))} \qquad (1)$$

As the fluctuations reside in the modulus and not in its phase angle, |G*|(t) was analysed, as this quantity is less scattered than G'(t) and G"(t). The resulting input data $G_{norm}(t)$ was analysed with the FFT routine of Matlab. Due to the constant frequency of 10 rad/s, |η*|(t) would show the same result, just factor 10 lower.

Results

Strain sweeps

The strain sweeps of the composites can be roughly put into two categories (Figure 2). PNI-GO3 (Figure 2a) and PNI-GO2 (Figure 2b) show a clear increase of G' and G" for $\gamma_0 \gtrsim 0.6\%$ followed by a peak at $\gamma_0 \approx 3.5\%$ and a secondary peak at $\gamma_0 \approx 10\%$. At higher deformations, γ_0, G'(γ_0) and G"(γ_0) decrease and δ(γ_0) increases, typical of the non-linear regime. While the principal shape of the strain sweep – a peak of both G'(γ_0) and G"(γ_0) – was previously observed for associative polymers,[55-57] it is novel to the authors that this kind of behaviour exists with δ(γ_0) being unaffected approximately up to the deformation where both G'(γ_0) and G"(γ_0) decrease sharply. The usual finding is that the peak in G'(γ_0) occurs at significantly smaller γ_0 than G"(γ_0)-peak.

Furthermore, associative polymer systems usually have a nonlinearity limit similar to regular polymer melts, i.e. around γ_0=30-50%.[55] This finding, however, is readily explained by the fact that a high surface area nanofiller is present in the composite, albeit in small concentrations. The data, nevertheless, clearly show that the interactions of GO and PNIPAM in the PNI-GO2 and PNI-GO3 samples are intensive enough to reduce the nonlinearity limit to about γ_0=0.6% with respect to G'(γ_0) and G"(γ_0) (with respect to δ(γ_0)' the nonlinearity limit would be about 7%). This is even more surprising, as an almost complete recovery of a creep deformation γ_c of 400% was previously found for PNI-GO3.[26]

The data of PNI-GO2 (Figure 2b) and PNI-GO3 (Figure 2a) differ slightly in phase angle, which, however, is also influenced somewhat by inertia of the sample, lowering δ slightly.

The data of PNI-RGO3 (Figure 2c) and PNI+GO3 blend (Figure 2d) show an approximately constant G'(γ_0) and G"(γ_0) up to γ_0=20%. PNI-RGO3 shows a small dip around 4%, which is exactly the onset of nonlinearity with respect to δ(γ_0). PNI+GO3 blend (Figure 2d) shows a very flat peak around γ_0=4% followed by a plateau at higher deformations. δ(γ_0) increases very slightly, but definitely not enough to call this the onset of nonlinearity. For this reason, we have to state that the PNI-RGO3 and PNI+GO3 blend have a significantly higher onset of nonlinearity than PNI-GO3, which suggests fundamental differences in the connectivity between the filler and PNIPAM, already highlighted in the steady-shear data, published separately.[26] These results differ significantly from the ones previously published on the same materials,[26] which is likely the consequence of varying test protocols. Ghavaminejad et al.[26] reported data on pre-sheared samples investigating the influence of the filler (and not the influence of the interactions between GO and PNIPAM), while for the data shown in Figure 2 the sample was not pre-sheared. The fact that for PNI-GO2, the nonlinearity limit without pre-shear (Figure 2b) is γ_0=0.4% with respect to G'(γ_0) and G"(γ_0), while the same indicators show a nonlinearity limit of γ_0=18% after pre-shearing indicates the importance of properly adjusting the shear history of samples.

These differences in nonlinear behaviour for the graphene-based filler and PNIPAM composite suggest significantly different structures from conventional nanocomposites, which can be seen, for example, from the disagreement in the established shapes of the strain sweeps as shown previously.[55] These results differ significantly from the data of pure PNI, which has been published elsewhere.[1] Pure PNI has a clear nonlinearity limit at $\gamma_0 \approx 30\%$ without any anomalies, such as peaks in G'(γ_0) or G"(γ_0), which is typical for polymer solutions. Furthermore, due to the lack of a structure building component in the material (GO or RGO), the phase angle δ is significantly higher in the linear regime than the *in-situ* synthesized composites.

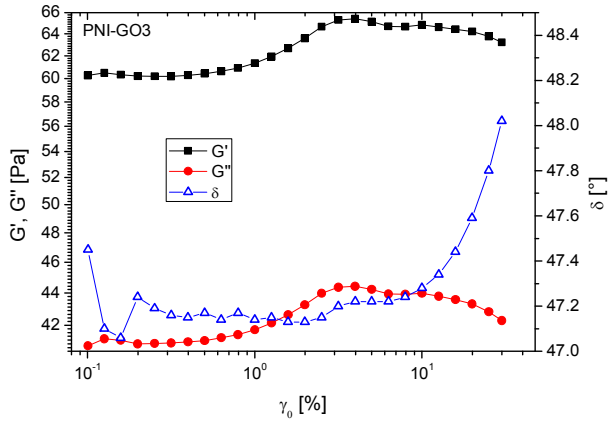

a)

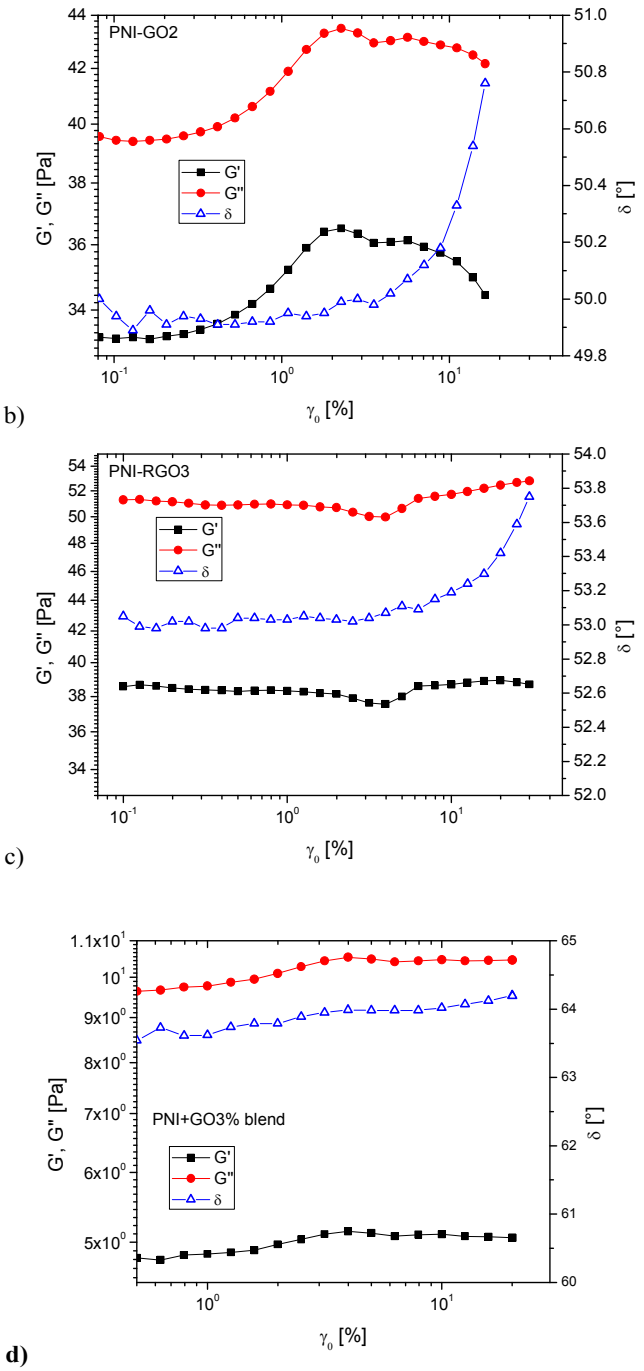

Figure 2: Strain sweeps of a) PNI-GO3, b) PNI-GO2, c) PNI-RGO3, and d) PNI+GO3 blend.

Recovery after shear

Figure 3 shows the comparison of the time sweep in the linear viscoelastic regime of PNI-GO3 after different deformations γ_0^{max}=5-30% in the strain sweep. While it is clear that the viscosity oscillates strongly for γ_0^{max}=5% and 10% (Figure 3a), the oscillations are much slower and weaker for γ_0^{max}=20% and 30%. On the other hand, it is obvious that the phase angle δ does not follow the same oscillations (Figure 3b). While it scatters somewhat (by about ±0.1°, which is not surprising due to the low modulus of the samples), it only shows a consistent trend towards lower δ with increasing time. Furthermore, it is clear that this trend is almost negligible for γ_0^{max}=5%, while the decrease is around 1.4° for γ_0^{max}=30%. This agrees qualitatively with the finding that viscosity increases overall in the same way.

The next question relates to the conditions, under which these oscillations occur. Figure 3a shows a comparison of the time sweeps after strain sweeps of γ_0^{max}=5%, 10%, 20%, and 30%, for which significant differences occur. These experiments were performed on the same sample starting at the lowest strain sweep deformation γ_0^{max} followed by a 10000 s time sweep. Throughout the test time, a water saturated atmosphere was ensured to avoid any sample changes due to evaporation of water. The lowest initial deformation in the strain sweep γ_0^{max}=5% leads to the abovementioned modulus oscillations without a long-term increase in viscosity. For higher initial deformations, increases in η_{begin}/η_{end} (defined as the difference between first and last point in the time sweep) by 6.0%, 10.0%, and 9.1% were found for γ_0^{max}=10%, 20%, and 30%, respectively. Furthermore, while the modulus oscillations are clearly visible for γ_0^{max}=10%, although with significantly slower and weaker oscillations, the oscillations are very weak for γ_0^{max}=20% and 30%. This behaviour qualitatively resembles data by Wu et al.[58] on fumed silica gels in dodecane and of Schmidt and Münstedt[59, 60] on glass particle suspensions in polyisobutylene. In these cases, it was discussed that a fractal network recovers from the strong shear (of loading the sample or actual rheological flows), thus, leading to an increase of viscosity with time. Our data shows similar trends, especially similar to Wu et al.[58] that the viscosity increases to different extents in the time sweep (in the linear range) after shear. However, while the viscosity increase with time agrees to literature, our materials show the above-mentioned oscillations, additionally. It is also clear that giving exact numbers of the increase is complicated by the viscosity oscillations.

Figure 3b shows the phase angle of the same dataset. It is clear that the increase in viscosity corresponds to a decrease in phase angle δ(t). For γ_0^{max}=5%, only a hardly significant decrease in phase angle Δδ (by about 0.1° on average) is found, which, as can be seen from Figure 3b, is about the same as the experimental accuracy of this quantity under the chosen experimental conditions. It remarkable, however, that, despite the clear oscillations in |η*|(t), δ(t) does not show any periodicity, which means that G'(t) and G"(t) run parallel to each other (Figure 3c). Hence, the processes causing the modulus oscillations do not leave a fingerprint in the phase angle, which is quite unusual, as almost all changes in rheological behaviour can be seen well in phase angle and, often, the phase angle shows the changes best.

It is also obvious from Figure 3b that the higher the deformation in the strain sweep, γ_0^{max}, the higher the decrease in phase angle Δδ. In comparison to η_{begin}/η_{end}, Δδ shows an even clearer relationship with γ_0^{max}. Hence, both |η*|(t) and δ(t) show that PNI-GO3 undergoes structural perfectioning after shearing at intermediate deformations.

Lower deformations in the strain sweep γ_0^{max} for this material did not lead to modulus oscillations, while for PNI-GO2 lower deformations (γ_0^{max}=3%) also yielded clear oscillations.

Based on this, it can be concluded that there are two effects that can occur when applying an intermediate deformation can produce oscillations in viscosity with constant or increasing periodicities and an increase in viscosity, which resembles many aspects of "shear-induced gelation by supramolecular

interaction".[45] Although it was not possible to reproduce the material behaviour within an error margin of 5%, the qualitative findings – occurrence of viscosity increase and modulus oscillations with comparable periodicity and amplitude – are reproducible.

For $\gamma_0{}^{max}$=5%, the data show a peculiar M-like or W-like shape and, furthermore, it is clear that the periodicity increases with time. Figure 3c shows the data of a different run for the same sample plotted on a logarithmic time scale, and it is obvious that for t>300 s, an approximately logarithmic constant periodicity is found, which will be analysed in greater detail later.

Considering these findings, it can be concluded that there are two overlapping effects. On the one hand, the modulus/viscosity oscillates after a slightly nonlinear deformation pulse, while at higher previously-applied deformations the oscillations become slower and weaker. However, a stronger nonlinear deformation leads to stiffer and more elastic behaviour, thus, indicating structural refinement.

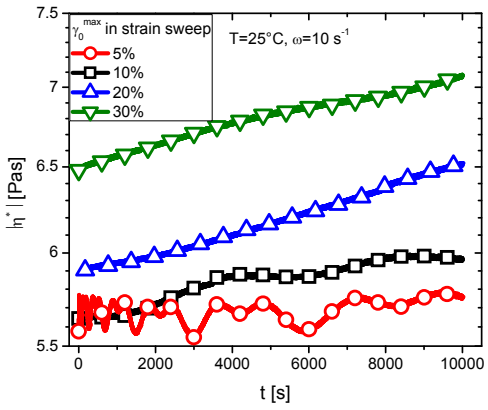

a)

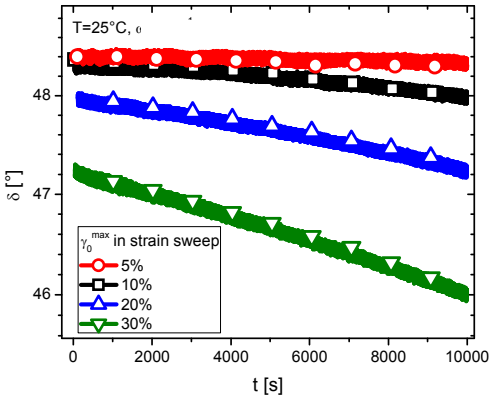

b)

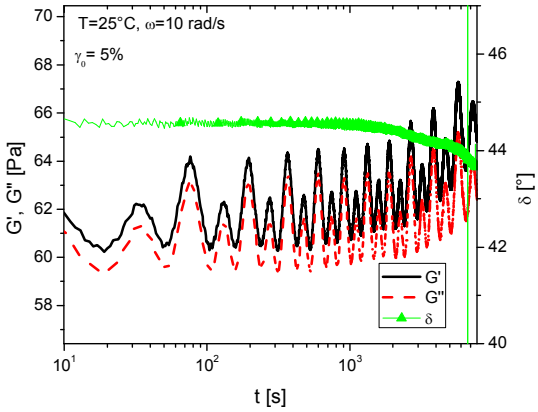

c)

Figure 3: Comparison of the viscosities of PNI-GO3 in the time sweep following a slightly nonlinear deformation $\gamma_0{}^{max}$=5-30% in the strain sweep. a) |η*|(t), b) δ(t), c) G'(t), G"(t), δ(t) for PNI-GO3 with log time scale. Shear stress σ_0=2 Pa, ω=10 rad/s, T=25°C.

Figure 4 shows the results for the same test setup as given in Figure 3 for PNI-RGO3. Figure 4a demonstrates the aforementioned structural perfectioning, but shows oscillations at a much higher frequency than that found for PNI-GO3. For PNI-GO3, the oscillations at $\gamma_0{}^{max}$=20% and 30% are so slow and weak that they are barely visible; for PNI-RGO3 a periodicity in the order of 100-300 s is found. At the same time, the data at $\gamma_0{}^{max}$=10% and especially 5% do not show clear signs of oscillations. However, when zooming in (Figure 4b), it becomes obvious that these data are also oscillating with a M- or W-like shape, but a much shorter periodicity, around 100 s, as opposed to several 1000 s for PNI-GO3.

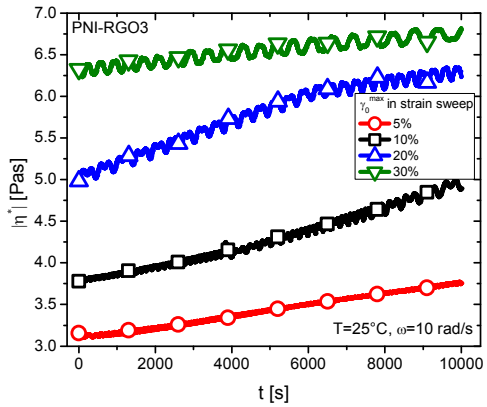

a)

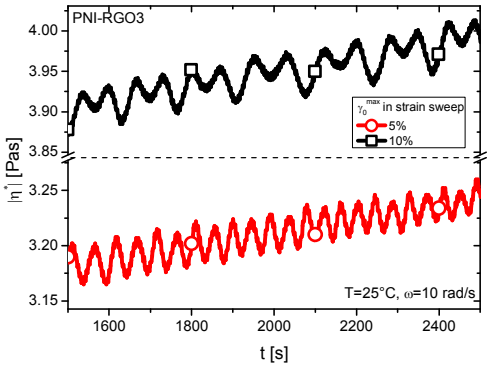

b)

Figure 4: Comparison of the viscosities of PNI-RGO3 in the time sweep following a slightly nonlinear deformation γ_0^{max}=5-30% in the strain sweep. A) |η*|(t), b) δ(t). Shear stress σ_0=2 Pa, ω=10 rad/s, T=25°C.

Most of the findings discussed so far concerned PNI-GO3, which makes one wonder how changes in sample composition and sample preparation affect the occurrence of the effects discussed above.

Figure 5 compares the time sweeps for PNI-GO2, PNI-GO3, PNI+GO3 blend and PNI-RGO3 for a total recovery time of 10000 s. PNI-GO2 behaves in a manner similar to PNI-GO3, however, the pattern observed here is significantly more complex than for the previous reports, as not only a M- or in some cases a W-like pattern is found (vs. a normal sinusoidal or saw-tooth-like pattern). Furthermore, the oscillation time changes for PNI-GO3, while for PNI-GO2 the amplitude of the oscillation varies; however, at a first glance, the oscillation period remains constant,[40, 41] which suggests that the concentration of GO plays a minor role once a certain threshold is reached; it should be mentioned that similar tests were also attempted for GO-contents below 2% and no modulus oscillations were observed. Furthermore, PNI-GO2 increases in viscosity with time, while PNI-GO3 does not show an overall increase. It is clear from Figure 5a that the PNI+GO3 blend does not lead to any oscillations beyond experimental accuracy. However, for larger deformations, i.e., γ_0^{max} between 20% and 100%, weak oscillations are found.

Clearly, these differences deserve a more detailed look with respect to when this effect happens and how it can be interpreted. The first obvious question is whether this is an artifact. Figure 5 shows five samples tested, which are rather comparable in viscosity. Test setup (rheometer, temperature, sample loading, and geometry) and method were exactly the same, so that an influence of these outer parameters can be excluded. This clearly suggests that the effect is related to material and not to imperfections in the experimental setup. The fact that only in-situ polymerised samples (PNI-GO2, PNI-GO3, PNI-RGO3) show oscillations, while the blended sample does not for γ_0^{max}=5%, suggests that the sample preparation method is decisive for the occurrence of oscillations. Additionally, a test performed on pure PNIPAM (PNI, diamond symbols) does not show any trace of systematic oscillations for γ_0^{max}=3-100%, while due to the low torque during the test clearly visible statistical scatter is obvious.

Furthermore, for several published examples on gels, which were done with the same test setup (alas with different γ_0^{max}), no such oscillations were observed.[61, 62]

Furthermore, it is obvious that for PNI+GO3 blend, the viscosity is lower than for pure PNI, which is counterintuitive. However, it can be easily explained by GO absorbing part of the PNIPAM on the surface, which decreases the effective concentration of PNIPAM in solution. On the other hand, few grafted chains exist, which makes bridging several GO-sheets unlikely and, thus, the gelation does not happen, which would counter the effect.

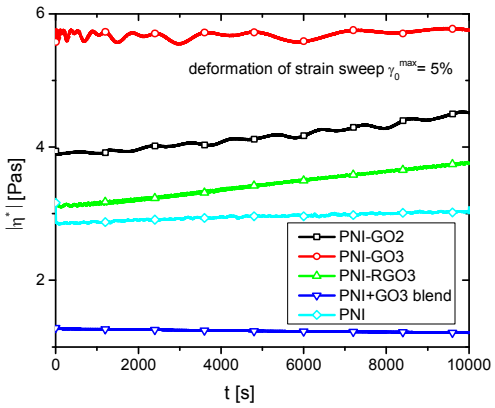

Figure 5: Comparison of the viscosities of PNI-GO2, PNI-GO3, PNI+GO3 blend, and PNI-RGO3 in the time sweep following a slightly nonlinear deformation γ_0^{max}=5% in the strain sweep. Shear stress σ_0=2 Pa, ω=10 rad/s, T=25°C.

So far, the discussion was limited to $\gamma_0^{max}\leq$30%. Figure 6 shows the data for PNI-GO3 for γ_0^{max}=100% (a) and 300% (b). Neither experiment shows any clearly visible periodic oscillations. However, for both materials, the data first goes through a maximum, for γ_0^{max}=100% the maximum is 137 s after the end of the high deformation, for 300% the maximum is at 269s. This is followed by a minimum 489 and 949 s after the end of the high deformation for 100% and 300%, respectively. While the time sweep after γ_0^{max}=100% leads to a significant increase after this minimum, the data for γ_0^{max}=300% only slightly exceeds the pre-deformation values.

This "wave" should not be mistaken for rheochaos and is straightforward to interpret by splitting the recovery into three phases. Firstly, the supramolecular interactions between GO and PNIPAM heal the microscopic cracks and broken connections, thus, significantly increasing G'(t) and G"(t). The dominant processes for the next step, decreasing G'(t) and G"(t), are oriented chains releasing their orientation, which have a higher stiffness than random coils. These orientations stem from random attachments of stretched chain segments to GO at high deformations. As the attachment is supramolecular with a short lifetime, taking away the high deformation leads to a recoiling of released chain segments and subsequently to a decrease of G'(t) and G"(t) in an exponential decay-like fashion, as can be seen from t=900-1300 s in Figure 6. The third process, following the first two, is a slow structural perfectioning due to the increase in the number of supramolecular connections between GO and PNIPAM. This increase is facilitated by the previous partial breaking up of the structure, which allows for a reattachment of PNIPAM on GO in a fashion, which has a higher fraction of attachments of a PNIPAM-chain covalently connected to one GO-sheet, but supramolecularly interacting with another one. Furthermore, the

previously described arguments about processes of rebuilding a hitherto destroyed fractal network also apply.[58-60]

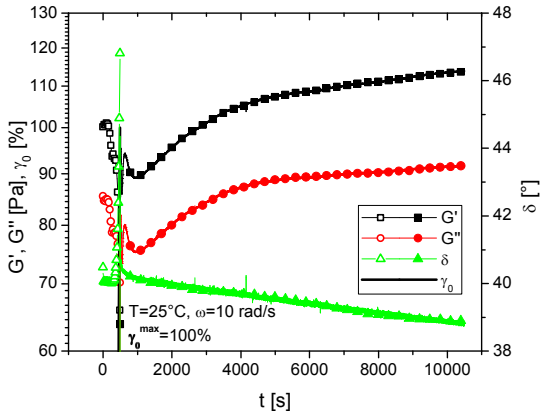

a)

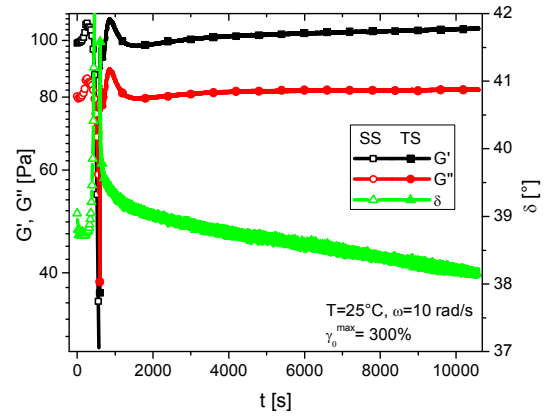

b)

Figure 6: Strain sweep and subsequent time sweep for PNI-GO3 for deformations γ_0^{max} of a) 100% and b) 300%. Shear stress in the time sweep (filled symbols) σ_0=2 Pa, ω=10 rad/s, T=25°C.

This structural perfectioning can also be observed for the other materials. Figure 7a shows that, for PNI-GO3, the increase of the deformation in the strain sweep γ_0^{max} leads to a monotonic increase of Δδ, while the viscosity change η_{end}/η_{begin} (calculated from the ratio of the last point of the recovery test to the one at the beginning (5s after start of the recovery phase) goes through a maximum around γ_0^{max}=100%. This suggests that a high deformations γ_0^{max} on one hand lead to a viscosity increase, but on the other hand inflicts so much damage on the sample that it limits the viscosity increase. The mechanism – probably an increase of viscosity due to increase in hydrogen bonding between PNIPAM and GO – is comparable to the "shear-induced gelation by supramolecular interaction" mechanism established earlier.[45] The decrease of δ, i.e. the increase of Δδ, is a clear confirmation of the strengthening of the network as ideal rubbers and gels tend to δ(ω)=0°, while covalently crosslinked hydrogels and supramolecular gels were found to have δ(ω) as low as 0.5-1.5° depending on the molecular structure and were nearly independent of frequency.[61, 63, 64] The continuous increase of Δδ for PNI-GO3 suggests that even a high deformation does not disrupt the network sufficiently to not make the network more elastic anymore.

When decreasing the amount of GO to 2% (Figure 7b), a quantitatively slightly different picture emerges. For the conditions tested, the increase in η_{end}/η_{begin} and even more in Δδ is more significant than for PNI-GO3. For PNI-RGO3 (Figure 7c), a decrease of η_{end}/η_{begin} and Δδ is found with a peak around γ_0^{max}=10%, while for PNI-GO3, the peak is at γ_0^{max}=100%. This difference suggests a significantly weaker bonding of PNIPAM on RGO than on GO, which is what would be expected from the understanding of the interactions.

The PNI+GO3 blend (Figure 7d) shows a similar behaviour to PNI-GO3, but the effects are much weaker especially with respect to η_{end}/η_{begin}. What also stands out is the fact that only for the blend, it was possible to disrupt the structure in the sense that the Δδ is negative/ η_{end}/η_{begin} is below 1, i.e. that viscosity and phase angle decrease and increase, respectively, in the recovery test after a shear pulse. What also sticks out that while the other samples show a change of about 25% in viscosity, the change is below +5% and -12% for the blend. This confirms the weak effects found for the PNI+GO3 blend by other rheological methods.

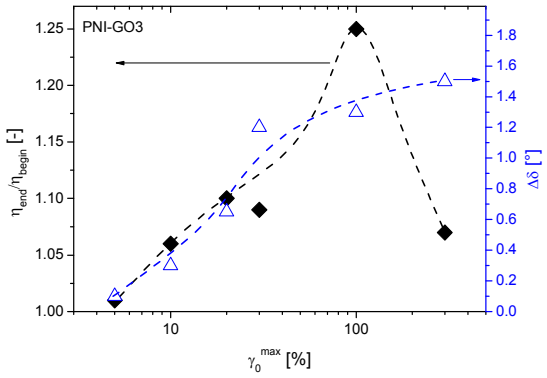

a)

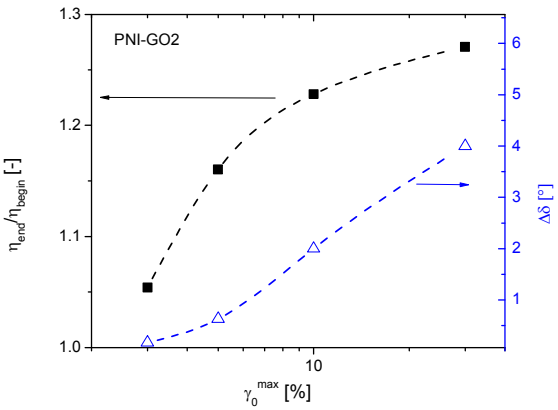

b)

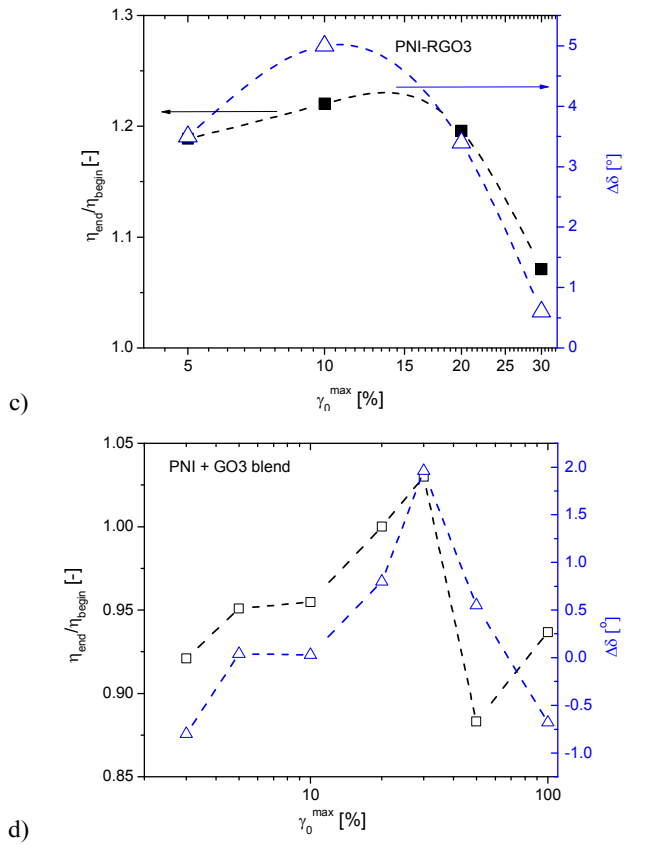

Figure 7: Viscosity ratio η_{begin}/η_{end} and phase angle changes Δδ for a) PNI-GO3, b) PNI-GO2, c) PNI-RGO3, and d) PNI+GO3 blend. The lines are added to guide the eye.

Spectral Analysis of Oscillations

Whenever a time series of wavy data is encountered, it is advisable to perform Fourier transformation of this data to check which kind of main frequencies are in the data. The necessary treatment of the data was described in the experimental section.

The FFT-power spectra of the different samples are given in Figure 8. All data have a peak at 0.2 Hz with an overtone of 0.4 Hz in common, stemming from the data acquisition rate of 1 point per second.

All samples tested under the different conditions show one or several main peaks between 10^{-4} and 10^{-2} Hz, which are distinctly stronger (i.e. have a larger integral area) than the abovementioned data spacing peak, indicating that the oscillations are significantly beyond the experimental inaccuracy.

Samples which showed a non-constant periodicity, such as PNI-GO3 with γ_0^{max} =5%, are obvious in Figure 8 by having a series of peaks in logarithmic equal spacing with a decreasing intensity with increasing frequency. Although it is clear that such datasets cannot be properly investigated with this method, the data is taken as is for the sake of comparison. The intensities of the oscillations are roughly the same for PNI-GO2 and PNI-GO3, somewhat weaker for PNI-RGO3, and much weaker for PNI+GO3 blend. In fact, the oscillations for PNI+GO3 blend are so weak that they can barely be detected when looking at the raw data (see SI). Hence, it is clear that in situ polymerisation plays a significant role in creating a structure responsible for this rheochaos. This finding also proves that the observed is not a mere experimental artefact, as sample composition, experimental setup and procedure are identical (except sample details).

For further analysis, the two highest peaks of each dataset (except the data spacing peak) were determined and compared in the following.

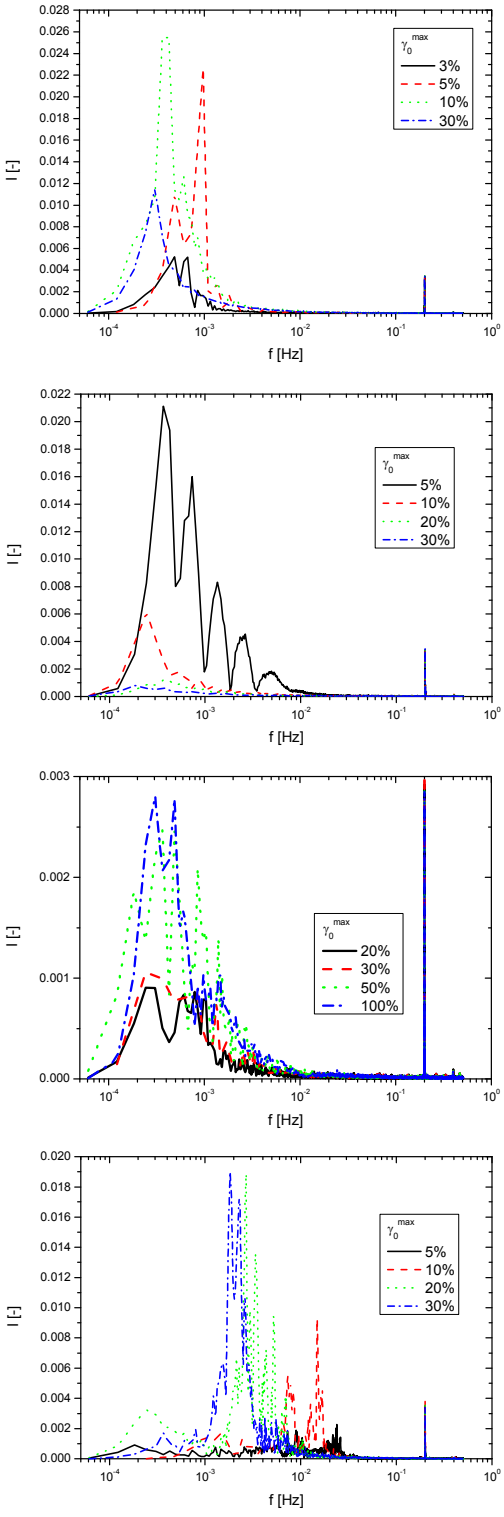

Figure 8: Fourier power spectra of a) PNI-GO2, b) PNI-GO3, c) PNI+GO3 blend, and d) PNI-RGO3.

The acquired maximum positions are plotted in Figure 9. It is clear that the two main frequencies (f_{max1} and f_{max2}) for the three GO-containing samples (PNI-GO2, PNI-GO3 and PNI+GO3 blend) are relatively similar (Figure 9a), while the oscillations of PNI-RGO3 are about a factor of 10 higher. This suggests that the governing mechanism for the oscillations is significantly different when using a graphene-based filler with fewer oxygen groups. Most likely, the smaller oxygen concentration leads to fewer interactions between tethered chains and oxygen-containing groups on the RGO in comparison to GO. Hence, the lower concentration of chains interacting supramolecularly with the RGO-sheets leads to shorter relaxation times, which in turn means that the oscillations can be faster.
Furthermore, it is clear that an increase in γ_0^{max} leads to a clear slowing down of the frequencies f_{max1} and f_{max2} of PNI-RGO3, while the same is not found for the other samples. However, it is not possible to deduce periodicities too low in frequency as the polynomial baseline will match the oscillations. For example, if the total experiment spanning 10000 s contains only 2-4 oscillations in total, these very slow oscillations of some of the experiments with the GO-containing samples would be difficult to observe.

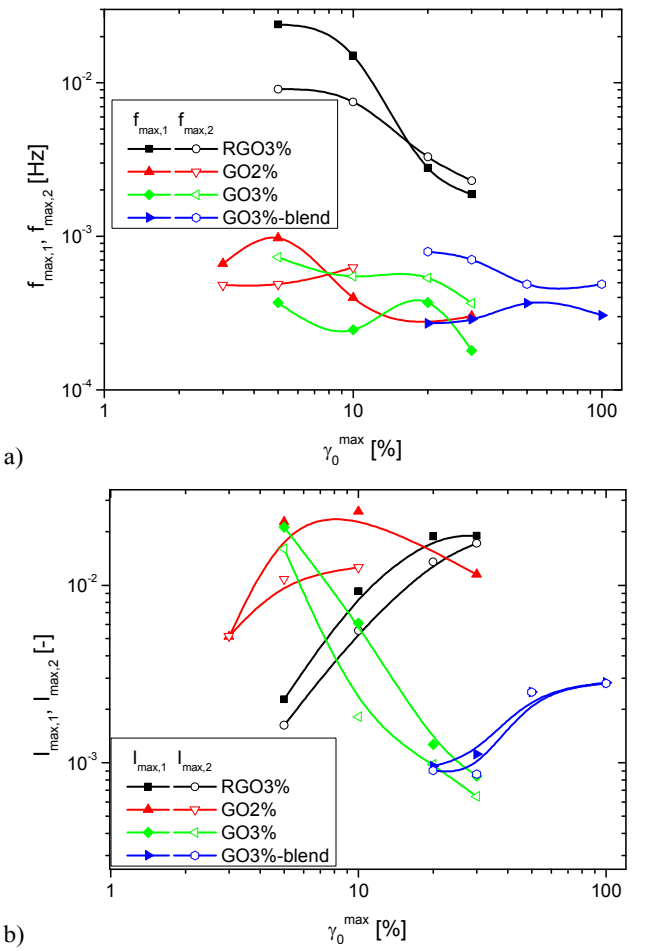

Figure 9: Frequencies (a) and intensities (b) of the strongest peaks as a function of applied deformation γ_0^{max} in the strain sweep experiment.

Figure 9b, however, shows that the oscillations are significantly less intense for the blend sample, indicating that this sample has significantly fewer interactions causing the oscillations.

Conclusions

Influence of composition

The behaviour observed in this article consists of rather unusual strain sweeps – stiffening under increasing strain (increase of $G'(\gamma_0)$ and $G''(\gamma_0)$) without a change in phase angle δ up to a nonlinearity limit. Furthermore, within this "abnormal" nonlinear range – for most samples studied in this article between γ_0^{max}=5 and 30%, a time sweep following this experiment leads to a variation of modulus (|G*|(t), G'(t), G''(t)), but not of phase angle δ, which usually slightly decreases as a function of time. These oscillations become slower the higher the previously applied deformation γ_0^{max}.
While the differences in rheochaos between 2% to 3% GO content are small, their macroscopic properties change significantly (viscoelastic liquid vs. highly elastic solid).[26] For GO concentrations below 2%, it was not possible to find any such oscillations, while for higher GO concentrations the material behaviour changes dramatically and leads to significant macroscopic phase separation.
Reducing the GO to RGO leads to significantly faster oscillations and smaller changes of viscosity and phase angle at medium and high deformations, which can be explained by fewer oxygen groups on the GO-surface to interact with the N-containing groups of the PNIPAM. Blending the PNIPAM-solution and GO instead of in-situ polymerisation leads to much weaker oscillations, which only occur at higher deformations γ_0^{max}.

Possible interactions in the material

Based on the previously drawn conclusions on these materials,[26] there are 4 potential interactions of the polymer chains in these systems (Figure 10):

1. H-bonding between N-containing groups in PNIPAM and O-containing moieties on the GO-sheets
2. Grafting of PNIPAM-chains on GO/RGO-sheets
3. Bridging of two GO/RGO-sheets by one chain
4. Entanglement interactions between two PNIPAM-chains tethered on GO/RGO-sheets

While the samples PNI-GO2 and PNI-GO3 have all of these interactions, PNI-RGO3 mostly lacks the possibility of tethered chains interacting with the oxygen on the surface (1), diminishing the process of chain adsorption, speeding up relaxation.
Blending instead of in-situ polymerising eliminates the possibility of grafting (2) and, hence, also the possibility of entanglement interactions of tethered chains (4) and bridging (3). However, it is possible to strongly adsorb chains temporarily, undergoing a supramolecular weaker version of processes (2, 3, 4), leading to weaker oscillations.

Comment: this scheme is new!

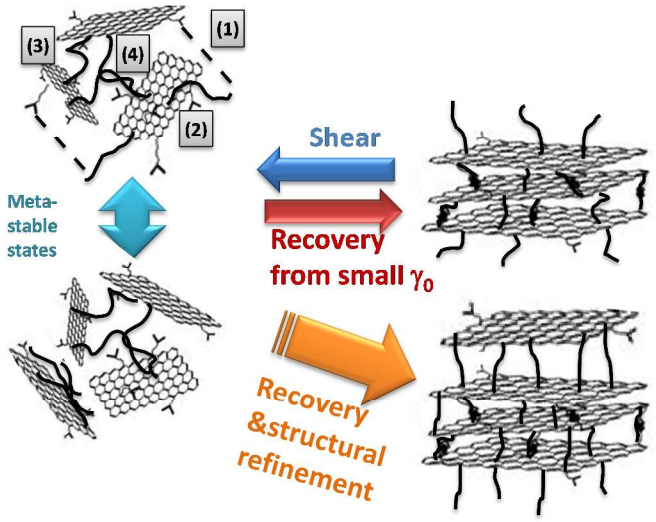

Figure 10: Schematic summarizing the different processes in the sample

Mechanism of the novel type of rheochaos

However, a question remains as to the mechanism causing the oscillations. The test protocol used for creating these oscillations is similar to ringing a bell – one strong ring can keep a bell ringing for some time. However, unlike the classical mechanical analogue under most conditions the oscillations do not stop within 3 h. As the longest retardation time of PNI-RGO3 is around 1 minute (determined from creep recovery[26]), it has to be concluded that something else keeps this process going because otherwise the oscillations would cease after several minutes at most.

The sample is strongly out of equilibrium when loading it into the rheometer, as the sample has to be squeezed into the shape provided by the geometry, which corresponds to a significant biaxial elongation coupled with a strong shear deformation.

As the data show, when shearing the sample, e.g. with γ_0^{max}=100% (Figure 6a), a significant increase in modulus becomes evident. As the same material does not show such an increase when only applying γ_0^{max}=5%, it is obvious that the shear leads to a stiffening of the sample, probably due to the alignment of the filler sheets increasing the modulus in shear direction orientation (and supposedly decreasing perpendicularly). Hence, the rheological properties of these materials are clearly shear history dependent.

As these changes in rheological properties require microscopic changes in the alignment of the fillers and their bonds with each other, distorting the structure by a deformation pulse might change the lowest energy configuration locally and metastably and the subsequent small oscillations are the trace of the different metastable states are fluctuating around an equilibrium (Figure 10). This would also explain why the fluctuations last much longer than the terminal relaxation time.

Stronger shear can reshuffle the network and allows for building a stronger structure, which can be observed as a significant modulus increase (Figure 6+Figure 10)

In the future, more advanced observation techniques and a better theoretical understanding of polymer-filler interactions, especially when using graphene based fillers, can lead to a deeper understanding of the dynamics behind this highly interesting and cryptic rheological behaviour.

Acknowledgements

The authors acknowledge financial aid from the National Research Foundation of Korea (110100713) and Nanshan District Key Lab for Biopolymers and Safety Evaluation (No.KC2014ZDZJ0001A). The authors would also like to thank the staff of the CBNU central lab especially Ms. Song-I Kim as well as Dr. Sungho Lee and his colleagues from KIST, Bongdong, Korea, for providing the GO.

References

[a]College of Materials Science and Engineering, Shenzhen University, Shenzhen 518060, PR China,
[b]Shenzhen Key Laboratory of Special Functional Materials, Shenzhen 518060, PR China,
[c]Shenzhen Engineering Laboratory for Advanced Technology of Ceramics, Shenzhen 518060, PR China
[d]Chonbuk National University, School of Semiconductor and Chemical Engineering, Baekjero 567, Deokjin-gu, Jeonju, Jeonbuk, 561-756, Republic of Korea
[e]Department of Chemical Engineering, NED University of Engineering & Technology, University Road, Karachi-75270, Pakistan
[f]Department of Bionanosystem Engineering, Graduate School, Chonbuk National University, Jeonju 561-756, Republic of Korea
[g]Nanshan District Key Lab for Biopolymers and Safety Evaluation, Shenzhen 518060, PR China
[h] BIN-fusion department, Chonbuk National University, Baekjero 567, Deokjin-gu, Jeonju, Jeonbuk, 561-756, Republic of Korea

*fjstadler@szu.edu.cn, Phone: +86-0755-26538236, Telefax: +86-0755-26536239, dongmei@jbnu.ac.kr
[#] These authors contributed equally

1. D. R. Dreyer, S. Park, C. W. Bielawski and R. S. Ruoff, *Chemical Society reviews*, 2010, **39**, 228-240.
2. A. Lerf, H. Y. He, M. Forster and J. Klinowski, *Journal of Physical Chemistry B*, 1998, **102**, 4477-4482.
3. S. Stankovich, D. A. Dikin, R. D. Piner, K. A. Kohlhaas, A. Kleinhammes, Y. Jia, Y. Wu, S. T. Nguyen and R. S. Ruoff, *Carbon*, 2007, **45**, 1558-1565.
4. F. Kim, L. J. Cote and J. Huang, *Adv Mater*, 2010, **22**, 1954-1958.
5. J. Luo, L. J. Cote, V. C. Tung, A. T. Tan, P. E. Goins, J. Wu and J. Huang, *J Am Chem Soc*, 2010, **132**, 17667-17669.
6. J. Kim, L. J. Cote, F. Kim and J. Huang, *J Am Chem Soc*, 2010, **132**, 260-267.
7. J. Kim, L. J. Cote, F. Kim, W. Yuan, K. R. Shull and J. Huang, *J Am Chem Soc*, 2010, **132**, 8180-8186.
8. O. C. Compton and S. T. Nguyen, *Small*, 2010, **6**, 711-723.
9. L. Q. Xu, W. J. Yang, K. G. Neoh, E. T. Kang and G. D. Fu, *Macromolecules*, 2010, **43**, 8336-8339.
10. J. I. Paredes, S. Villar-Rodil, A. Martinez-Alonso and J. M. D. Tascon, *Langmuir : the ACS journal of surfaces and colloids*, 2008, **24**, 10560-10564.
11. M. Fang, K. G. Wang, H. B. Lu, Y. L. Yang and S. Nutt, *Journal of Materials Chemistry*, 2010, **20**, 1982-1992.
12. C. S. Shan, H. F. Yang, D. X. Han, Q. X. Zhang, A. Ivaska and L. Niu, *Langmuir : the ACS journal of surfaces and colloids*, 2009, **25**, 12030-12033.

13. H. J. Salavagione and G. Martinez, *Macromolecules*, 2011, **44**, 2685-2692.
14. I. W. Hamley, *Introduction to Soft Matter: Synthetic and Biological Self-Assembling Materials*, John Wiley & Sons Ltd, Chichester, UK 2007.
15. B. J. Hong, Z. An, O. C. Compton and S. T. Nguyen, *Small*, 2012, **8**, 2469-2476.
16. S. M. Zhu, J. B. Li, Y. H. Chen, Z. X. Chen, C. X. Chen, Y. Li, Z. W. Cui and D. Zhang, *J Nanopart Res*, 2012, **14**.
17. Y. F. Yang, X. H. Song, L. Yuan, M. Li, J. C. Liu, R. Q. Ji and H. Y. Zhao, *J Polym Sci Pol Chem*, 2012, **50**, 329-337.
18. J. J. Qi, W. P. Lv, G. L. Zhang, F. B. Zhang and X. B. Fan, *Polymer Chemistry*, 2012, **3**, 621-624.
19. J. Dong, J. Weng and L. Z. Dai, *Carbon*, 2013, **52**, 326-336.
20. A. R. Payne, *Journal of Applied Polymer Science*, 1962, **6**, 57-63.
21. L. Hollaway, *Handbook of Polymer Composites for Engineers*, Woodhead Publishing, 1994.
22. P. Schexnailder and G. Schmidt, *Colloid and Polymer Science*, 2009, **287**, 1-11.
23. S. Thomas, K. Joseph, S. K. Malhotra, K. Goda and M. S. Sreekala, eds., *Polymer Composites, Volume 1, Macro- and Microcomposites*, Wiley, 2012.
24. H. Muenstedt, N. Katsikis and J. Kaschta, *Macromolecules*, 2008, **41**, 9777-9783.
25. A. Papon, H. Montes, F. Lequeux and L. Guy, *J Polym Sci Pol Phys*, 2010, **48**, 2490-2496.
26. A. GhavamiNejad, S. Hashmi, H. I. Joh, S. Lee, M. Vatankhah Varnoosfaderani, Y. S. Lee and F. J. Stadler, *Physical Chemistry Chemical Physics*, 2014, **16**, 8675-8685.
27. R. D. Priestley, C. J. Ellison, L. J. Broadbelt and J. M. Torkelson, *Science*, 2005, **309**, 456-459.
28. Z. Ye, S. Zhu and J. F. Britten, *Macromolecular rapid communications*, 2006, **27**, 1217-1222.
29. F. E. Antunes, L. Gentile, L. Tavano and C. O. Rossi, *Appl Rheol*, 2009, **19**, 42064-42069.
30. H. G. Schild, *Progress in Polymer Science*, 1992, **17**, 163-249.
31. F. O. Obiweluozor, A. GhavamiNejad, S. Hashmi, M. Vatankhah-Varnoosfaderani and F. J. Stadler, *Macromolecular Chemistry and Physics*, 2014, **215**, 1077-1091.
32. F. Hofmeister, *Archiv fuer experimentelle Pathologie und Pharmakologie*, 1888, **24**, 247-260.
33. G. S. Georgiev, E. B. Karnenska, E. D. Vassileva, I. P. Kamenova, V. T. Georgieva, S. B. Iliev and I. A. Ivanov, *Biomacromolecules*, 2006, **7**, 1329-1334.
34. M. Das, N. Sanson and E. Kumacheva, *Chemistry of Materials*, 2008, **20**, 7157-7163.
35. T. Friedrich, B. Tieke, F. J. Stadler, C. Bailly, T. Eckert and W. Richtering, *Macromolecules*, 2010, **43**, 9964-9971.
36. T. Friedrich, B. Tieke, F. J. Stadler and C. Bailly, *Soft Matter*, 2011, **7**, 6590–6597.
37. Y. Tamai, H. Tanaka and K. Nakanishi, *Macromolecules*, 1996, **29**, 6750-6760.
38. M. Y. Arica, H. A. Oktem, Z. Oktem and S. A. Tuncel, *Polymer International*, 1999, **48**, 879-884.
39. H. Senff and W. Richtering, *Colloid and Polymer Science*, 2000, **278**, 830-840.
40. M. A. Fardin, T. Divoux, M. A. Guedeau-Boudeville, I. Buchet-Maulien, J. Browaeys, G. H. McKinley, S. Manneville and S. Lerouge, *Soft Matter*, 2012, **8**, 2535-2553.
41. L. Gentile, B. F. B. Silva, S. Lages, K. Mortensen, J. Kohlbrecher and U. Olsson, *Soft Matter*, 2013, **9**, 1133-1140.
42. R. Ganapathy and A. K. Sood, *Phys Rev Lett*, 2006, **96**, 108301.
43. V. Lutz-Bueno, J. Kohlbrecher and P. Fischer, *Rheologica Acta*, 2013, **52**, 297-312.
44. J. B. Salmon, A. Colin and D. Roux, *Physical review. E, Statistical, nonlinear, and soft matter physics*, 2002, **66**, 031505.
45. T. Mahmoudi, V. Karimkhani, G. S. Song, D. S. Lee and F. J. Stadler, *Macromolecules*, 2013, **46**, 4141-4150.
46. M. Das, B. Chakrabarti, C. Dasgupta, S. Ramaswamy and A. K. Sood, *Physical review. E, Statistical, nonlinear, and soft matter physics*, 2005, **71**, 021707.
47. H. Münstedt, M. Schmidt and E. Wassner, *Journal of Rheology*, 2000, **44**, 413-427.
48. H. Palza, I. F. Naue and M. Wilhelm, *Macromolecular rapid communications*, 2009, **30**, 1799-1804.
49. I. J. Rao and K. R. Rajagopal, *Acta Mech*, 1999, **132**, 209-219.
50. M. Hirata, T. Gotou, S. Horiuchi, M. Fujiwara and M. Ohba, *Carbon*, 2004, **42**, 2929-2937.
51. C. Bartolini, L. Mespouille, I. Verbruggen, R. Willem and P. Dubois, *Soft Matter*, 2011, **7**, 9628-9637.
52. H. Chen, W. Li, H. Zhao, J. Gao and Q. Zhang, *Journal of colloid and interface science*, 2006, **298**, 991-995.
53. H. Yamauchi and Y. Maeda, *The journal of physical chemistry. B*, 2007, **111**, 12964-12968.
54. X. H. Wang, X. P. Qiu and C. Wu, *Macromolecules*, 1998, **31**, 2972-2976.
55. H. G. Sim, K. H. Ahn and S. J. Lee, *Journal of Non-Newtonian Fluid Mechanics*, 2003, **112**, 237-250.
56. P. Guillet, C. Mugemana, F. J. Stadler, U. S. Schubert, C.-A. Fustin, C. Bailly and J.-F. Gohy, *Soft Matter*, 2009, **5**, 3409.
57. K. Hyun, S. H. Kim, K. H. Ahn and S. J. Lee, *J. Non-Newtonian Fluid Mech.* , 2002, **107** 51-65.
58. X.-J. Wu, Y. Wang, M. Wang, W. Yang, B.-H. Xie and M.-B. Yang, *Colloid and Polymer Science*, 2011, **290**, 151-161.
59. M. Schmidt and H. Münstedt, *Rheologica Acta*, 2002, **41**, 205-210.
60. M. Schmidt and H. Münstedt, *Rheologica Acta*, 2002, **41**, 193-204.
61. M. Vatankhah-Varnoosfaderani, A. Ghavaminejad, S. Hashmi and F. J. Stadler, *Chemical communications*, 2013, **49**, 4685-4687.
62. M. Vatankhah-Varnoosfaderani, S. Hashmi, A. GhavamiNejad and F. J. Stadler, *Polymer Chemistry*, 2014, **5**, 512.
63. J. D. Ferry, *Viscoelastic Properties of Polymers*, John Wiley and Sons, New York, 1980.
64. S. Hashmi, A. GhavamiNejad, F. O. Obiweluozor, M. Vatankhah-Varnoosfaderani and F. J. Stadler, *Macromolecules*, 2012, **45**, 9804-9815.